A Simple Planar Micromixer with Low Pressure Drop For Disposable Lab-on-a-Chip (LOC) Systems

Ali Asgar S. Bhagat, Erik T.K. Peterson and Ian Papautsky

Department of Electrical and Computer Engineering,
University of Cincinnati, Cincinnati, OH

ABSTRACT

In this work the design and fabrication of a novel passive microfluidic mixer capable of achieving mixing in shorter distances and lower Reynolds numbers (*Re*) is reported. Passive mixers typically rely on the channel geometry to mix fluids, and many previously reported designs work efficiently only at moderate to high *Re* and are often difficult to fabricate as they incorporate complex 3-D structures within the channel. The mixer design discussed in this work achieves good mixing at low *Re*, has planar geometry and thus is simpler to fabricate and integrate with existing lab-on-a-chip (LOC) technologies. The design incorporates triangular notches patterned along the channel walls to laminate the flow, thus enhancing mixing. Numerical and experimental studies to determine the effect of the notch dimensions and placement within the microchannel were carried out to optimize the mixing performance. Results show that the final mixer design is efficient at mixing fluids at low *Re*. The mixer is fabricated in polydimethylsiloxane (PDMS) bonded to glass slides and tested using fluorescence dyes. Results show that the new design exhibit complete mixing at $Re < 0.1$ within 7 mm and thus will benefit a wide range of LOC applications where space is limited.

Keywords: Microfluidics, micromixer, CFD, modeling, microfabrication, lab-on-a-chip

1. INTRODUCTION

The multidisciplinary field of microfluidics studies the behavior of fluids at the microscale and mesoscale. The burgeoning due to the emergence of the concept of lab-on-a-chip (LOC) has revolutionized the microelectromechanical systems (MEMS) community, especially microfluidics. Miniaturization of analytical systems offers many advantages, such as increased throughput, reduced analysis time, reduced quantity of expensive reagents, improved accuracy, integrated reference standards, reduced contamination due to low-cost disposable devices, and increased portability.[1-3] For many of these miniaturized biological systems mixing is needed in microchannels for blending, emulsification and suspensions of two or more fluids, and mixing of reactants for process initiation in applications such as enzyme assays[4], DNA restriction fragment analysis[5], DNA sequencing[6], PCR amplification[7-9], electrophoretic analysis[10-12], and cell separation and lysis.[13,14]

Due to their small size, microchannel flows are typically characterized by low *Re* of the order of 1 or less. Reynolds number (*Re*) is a non-dimensional parameter that compares the inertial forces to viscous forces. At lower *Re* viscous forces are dominant and inertial forces are negligible making molecular diffusion the predominant mixing mechanism resulting in longer mixing lengths. Micromixers are broadly classified as active and passive, based on the mixing mechanism. Active mixers have moving parts inside the channel, while passive mixers do not have any moving parts and rely completely on microchannel geometry. Due to their complex fabrication, high cost, need for active control and typically high power consumption, active mixers are not generally preferred for LOC applications, thus establishing a clear need to develop better passive mixers to fully exploit capabilities of existing LOC technologies.

One of the primary factors for achieving fast mixing in passive micromixers is to ensure that the two fluids are interspersed such that the area of contact between them increases thereby allowing faster diffusion. While designing these micromixers one needs to keep in mind the characteristics of a good micromixer such as small mixing lengths, simpler fabrication and integration with existing LOC technologies, and efficient mixing at $Re < 1$. Other important characteristics that are generally overlooked while designing these mixers are – limiting pressure drop to enable cascading these devices, and simple mixing mechanisms that do not cause damage to biological samples such as

Microfluidics, BioMEMS, and Medical Microsystems V, edited by Ian Papautsky, Wanjun Wang,
Proc. of SPIE Vol. 6465, 64650A, (2007) · 0277-786X/07/$15 · doi: 10.1117/12.698370

blood and cell suspensions. A recent article by Nguyen and Wu[15] reviews the different micromixers (both active and passive) that have been reported to date. The review discusses in detail the different mixing mechanisms and examples employing them.

Some of the early work in the field of micromixers was performed by Branebjerg *et al.*[16] who developed a mixer based on the principle of multi-stage multi-layer lamination of two fluids. The mixer split flow into N substreams and then recombined them into a single stream with 2^N layers. To enhance mixing, the thickness of laminae was varied periodically by passing them through narrow slits in the channel. Later, Liu *et al.*[17] successfully demonstrated passive mixing using lamination and transverse momentums by employing bends in microchannels. The "C-shaped" units were used to introduce chaotic advection thereby enhancing mixing. Chaotic advection is present when particles in a flow move in adverse directions relative to the typical flow and in effect increase the surface area and the diffusion of the mixing fluids. Each time a fluid flows through a C-shaped unit, it is rotated by 90^o in either the clockwise or counter clockwise direction. By repeatedly rotating the fluid in either way a rotating component to an otherwise laminar flow is added, resulting in mixing.

The concept of chaotic advection was further developed by Stroock *et al.* [18] when a series of patterned base relief structures were used to introduce chaotic behavior into a microchannel. The patterned grooves introduced a rotational component to the fluid flow. Introducing asymmetry between the herringbone shaped grooves break-up the flow increasing the mixing efficiency and decreasing the effective mixing length. By varying the degree of asymmetry and the amplitude of rotation of the fluids, mixing could be controlled. Kim *et al.* [19] further modified the herringbone channel by inserting barriers along the top surface of the channel along with the slanted grooves on the bottom surface. The slanted grooves along the bottom of the channels produced helical flows which are characterized by a single elliptic point. The barriers along the channel top surface split helical flow into two co-rotating streams characterized by a single hyperbolic point and introduced periodic perturbations in the velocity of the two fluid streams. Recently, Hong *et al.* [20] introduced a novel micromixer based on the Coanda effect. Coanda effect is the tendency of a stream of fluid to stay attached to a convex surface, rather than follow a straight line in its original direction.[21] The mixer consisted of modified Tesla structures to produce flows in the transverse direction and offsetting them forced one fluid stream into the other alternately causing mixing.

However, the above mentioned designs suffer from one or more of the following disadvantages: (i) the designs incorporate three dimensional features which require multi-step lithography, making the fabrication complex and time consuming; (ii) the mixing mechanism employed may potentially damage biological samples such as cell suspensions or blood; (iii) although the designs are quite efficient in the $1 < Re < 100$ range, they are still not very efficient at low Re ($Re < 1$). In this paper, we report on a new passive microfluidic mixer with low pressure drop for disposable LOC systems, capable of mixing at short distances for low Re (< 0.1) flows.

2. DESIGN AND MODELING

2.1 Design

The micromixer concept is illustrated in Figure 1, and consists of alternating triangular features, protruding into the center of the channel to alternately force one fluid stream into the other. This alternating action of the two fluids results in mixing. It is important to note that the notches resemble right triangles rather than isosceles triangles. While modeling, it was determined that the right triangular shaped notches performed better than isosceles shapes. There may be several reasons for this. Small vortices are induced at the sharp tips of the features and higher velocities are also observed in this region when compared to a symmetrical, isosceles shaped feature. Also, by eliminating the right halves of the features, more notches can be packed into a given distance, thus achieving faster mixing. The design is similar to the zig-zag channel reported by Branebjerg *et al*.[22] In this work we investigate the effects of this triangular sidewall geometry on mixing. The three control parameters examined were: notch length (L), notch width (W), and spacing between consecutive notches (S) (Figure 1). To optimize the design, the effect each parameter mentioned above has on mixing was studied. The notch length was varied from 0 (*i.e.*, no notches) to 100 μm (*i.e.*, half channel width). The width was varied from 25 μm to 100 μm while the spacing was varied from 25 μm to 150 μm.

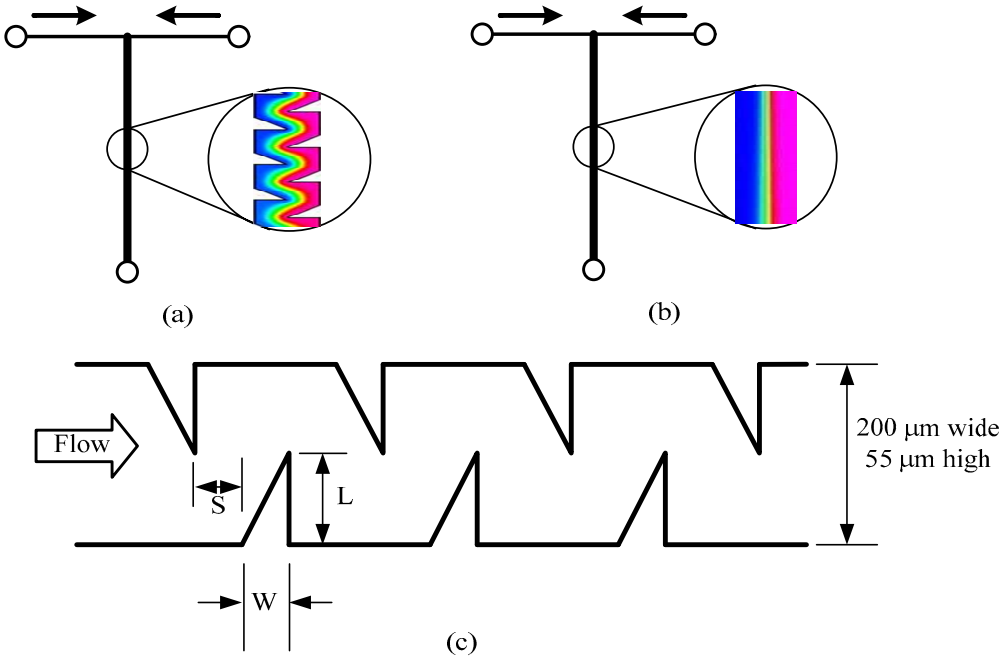

Figure 1. (*a*) Schematic representation of the micromixer with sidewall notches, (*b*) Conventional T-mixer, (*c*) proposed micromixer with notches illustrating key features and dimensions. The channel is 200 μm wide and 55 μm deep.

2.2 Micromixer Modeling and Simulations

The micromixer designs were modeled using the CFD-GEOM software and then simulated using the CFD-ACE+ software (ESI-CFD Inc., Huntsville, AL). To minimize the effect of meshing on mixing, the mesh density was continually increased until it had minimal effects on mixing. The computational domain was discretized with structured grids, approximately 60,000 cells per design, with majority of cells having all sides less than 5 μm. Meshing was aligned in the direction of flow.

The simulation environment was verified for steady incompressible flows. The physical properties of water were applied to the two fluids in the simulation; the density was set to 1000 kg/m^3 and the dynamic viscosity was set to 10^{-3} kg/ms. A diffusion co-efficient of 10^{-10} m^2/s was used for all the simulations. The velocity of the two species at the inlet was calculated for $0.01 \leq Re \leq 100$ (*i.e.*, 0.12 mm/s ≤ u ≤ 1200 mm/s), while the outlet was set to a fixed-pressure boundary condition. While modeling, setting the molar concentration of one of the fluid species to 0 and the other to 1 helped us to define the mixing length. The Algebraic MultiGrid (AMG) solver was used for pressure corrections while the Conjugates Gradient Squared (CGS) and Preconditioning (Pre) solver were used for velocity and species correction. The convergence limit for mass fraction was set to 10^{-6} and the simulations were run for 300 iterations.

CFD-VIEW was used to view the simulation results and calculate mixing percentages based on molar concentrations of the two fluids at any given length along the channel. At the entrance the molar intensity across half the channel is 1 while that of the other is 0. As mixing takes place the molar intensity on one side of the channel keeps decreasing while on the other side it keeps increasing. Complete mixing was said to be achieved when the molar intensity of the two fluids reaches 0.5. To quantify mixing, the standard deviation of the molar concentration distribution (pixel intensity distribution in the case of experimental characterization) is measured in the images of the cross-section of the channel at varying distances from the entrance as shown in Equation 1.

$$\sigma = < (I - < I >)^2 >^{\frac{1}{2}} \qquad (1)$$

where I is the gray scale pixel intensity and $< I >$ is the average overall the pixels in the image.[18] The pressure drop along the channel was also recorded for the various models.

3. EXPERIMENTAL METHODS

3.1 Micromixer Fabrication

Initially, 3" silicon wafers were cleaned with acetone, methanol and DI water for 3 min each. The wafers were then cleaned in piranha (7:3 H_2SO_4:H_2O_2, v/v) for 10 min. Following piranha clean, wafers were rinsed in DI water, dipped in BOE (Buffered Oxide Etchant), and rinsed once more with DI water. Wafers were dehydrated on a hotplate at 150 °C for 20 min before spin coating. Wafers were then coated with a thick negative photoresist, SU-8 2075 (MicroChem Corp.) to define the microchannels. For a 55 μm thickness, wafers were ramped to 500 rpm at 100 rpm/sec and held for 10 sec before ramping to 2700 rpm at 300 rpm/sec and held for 30 sec. After spin coating, wafers were transferred to a level surface for 10 min to allow the photoresist to relax. The pre-bake was performed on a level hot plate at 65 °C for 10 min and then ramped to 95 °C and held for 45 min, and finally cooled to room temperature. The resist was then exposed at 175 mJ/cm^2 using a high-pass filter to remove any deep UV. Post exposure bake was then carried out on a hotplate at 65 °C for 5 min and then at 95 °C for 10 min. The wafers were then developed using SU-8 developer, rinsed with isopropyl alcohol to confirm the development, and blown dry using N_2. Following development, patterned wafers were descummed in O_2 plasma for 3 min at 300 W.

Next, wafers were treated with Sigmacote (Cat # SL-2, Sigma-Aldrich) to facilitate release of the polydimethylsiloxane (PDMS) (Sylgard 184, Dow Corning) from the photoresist molds. The PDMS was mixed at a 10:1 (m/m) ratio of base to curing agent, degassed and then poured over the SU-8 molds to obtain a thickness of 1mm and cured at 80°C for 2.5 hrs on a level hotplate. The PDMS was then peeled from the SU-8 masters, and holes for inlets and outlets were punched before the PDMS molds were bonded to glass microscope slides (1"x3"). Bonding was performed by first cleaning both pieces in 1:5 (v/v) HCl/H_2O and then exposing the surfaces to O_2 plasma (20 sccm, 13.56 MHz) for 15 sec at 70 W.[23] Following plasma treatment, the surfaces were immediately brought into contact and placed on a hotplate at 85°C for 2 hrs to complete the bonding. The height and width of the fabricated channels was measured using a profilometer P-11 (KLA Tencor) and were found to be 55 μm and 200 μm respectively. Rounding of sharp corners for the notches was observed in the fabricated devices. This rounding meant that the notches did not go half way into the channel. The fabricated notches were ~90 μm in length rather than 100 μm which creates a 20 μm wide area in the center of the channel where no features were present. Also due to the absence of these sharp corners, regions of high vortices that were seen during simulations would not be present while characterizing this design experimentally. The effect of these fabrication limitations on mixing is discussed later.

3.2 Characterization

The devices were tested using a custom Plexiglas fixture designed in our laboratory. Using our fixture, tubing can be quickly and easily connected to the inlets and outlets reducing fabrication time and effort. Mixing was characterized using fluorescence microscopy.[24] When testing, one syringe was filled with a 1×10^{-6} M solution of fluorescein in DI water, and the other filled with DI water only. The two syringes were driven by syringe pumps, (New Era Pump Systems, NE-1000) at flow rates ranging from 0.2 μL/min to 100 μL/min. Mixing was observed using an inverted epifluorescence microscope (Nikon TE-2000) with a 16 bit CCD camera. Experimental set-up to characterize the micromixer is shown in Figure 2. Images were acquired and analyzed using Metamorph software (Universal Imaging). Images of the channel are captured and grey-scale line scans across the channel width are then recorded. Using the grey-scale values, mixing percentages can then be calculated using the techniques described in Section 2.2.

4. RESULTS AND DISCUSSION

4.1 Modeled Results

Simulations for the mixer with notches were performed for steady, incompressible flows for $Re = 0.1$ which is representative of typical microflow conditions. All the results discussed in this section are representative of 5 mm long channel. The notches within the microchannels do not cause any chaos in the fluid flow, but simply pushes the two streams into one another thereby facilitating diffusion to occur faster. To optimize the dimensions of these notches for efficient mixing, we look at the effect of three parameters, specifically, the notch length, width and the spacing between notches.

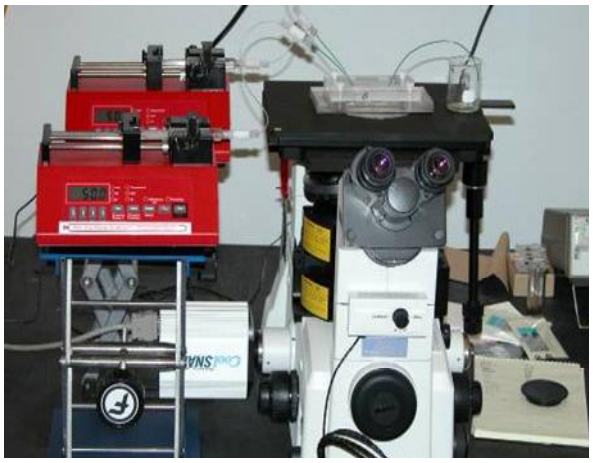

Figure 2. Photograph of the experimental set-up showing the microscope, syringe pumps and the microfluidic device fitted in the interconnect.

Notch length (L)

To optimize the mixer with notches, the effect the length of the notches has on mixing was investigated first. The length was varied from 0 μm to 100 μm with the width fixed at 50 μm and the spacing at 50 μm. The mixers with these various configurations were modeled and the simulation results are shown in Figure 3*a*, indicating that as the length of the notches is increased, so does the mixing. The lengths of the notches were not increased beyond 100 μm since it would result in much higher pressure drops (> 1 kPa) due to the reduced channel cross-section. Also, longer notches may result in dead volumes or recirculation regions near the sidewalls of the channel prohibiting the participation of the two fluids in mixing.

Notch width (W)

The width of the notches was varied from 0 μm to 100 μm with the length fixed at 100 μm and 50 μm spacing. Figure 3*b* shows the simulation results for varying widths. It appears that as the width of the notches is increased from 0 μm (no notches - T-mixer) to 25 μm, there is sudden increase in the mixing. Beyond 25 μm, the mixing gradually falls as the number of notches that can be packed within 5 mm decreases.

Notch spacing (S)

The spacing between the notches was varied from 25 μm to 150 μm with length fixed at 100 μm and width at 50 μm. The results shown in Figure 3*c* indicate that as the spacing between notches increases, the mixing decreases. This again is due to the fact that for a given length, more notches can be packed at shorter spacing than wider spacing. With the number of notches increasing for a given length, the fluids are pushed into each other often resulting in faster mixing.

Performance for varying Reynolds number (*Re*)

After analyzing the modeling data the optimized mixer was then modeled. Based on modeling results, the optimized mixer was designed to have 25 μm wide notches, spaced 25 μm apart and going half way into the channel. The optimized mixer was then modeled for varying *Re*. An interesting result was observed when the mixer was modeled for varying *Re* (Figure 7). At lower flow rates, since diffusion is the primary mixing mechanism greater mixing was observed. However, as the flow rate was increased, the mixing decreased until an inflection point is reached. Beyond the inflection point (*Re* = 1), the mixing increases with increasing flow rate. This can be explained by the fact that the mixing mechanism now is more convective based rather than diffusion based. From Figure 7, it can be seen that the performance of our mixer is different from that of a conventional T-mixer where the mixing keeps decreasing with increasing *Re* for a fixed channel length.

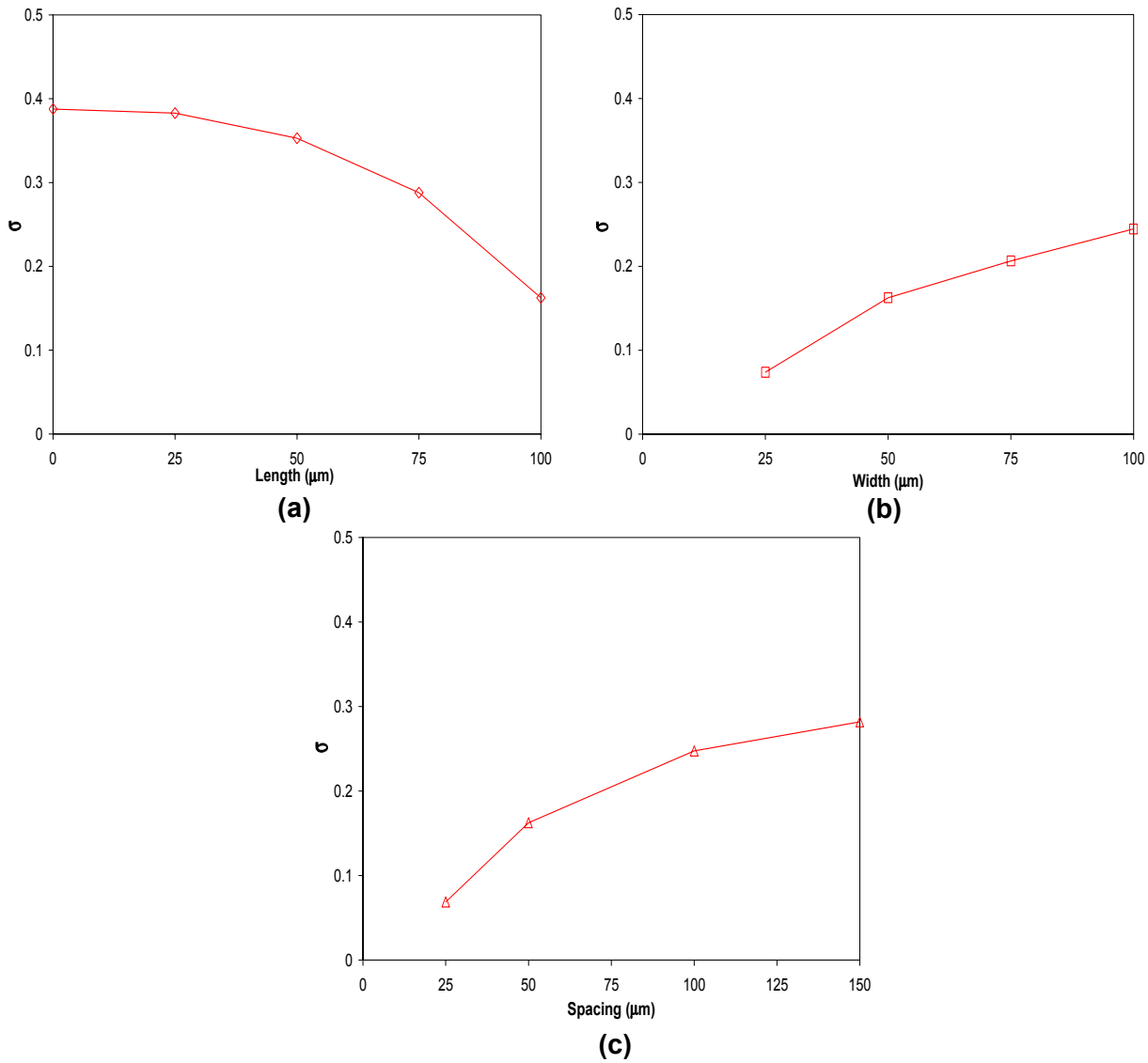

Figure 3. Mixing at 5 mm from the channel entrance for increasing (*a*) length of the notches with the width = 50 μm and spacing = 50 μm. (*b*) width of the notches with length = 100 μm and spacing = 50 μm. (*c*) spacing between the notches with length = 100 μm and width = 50 μm.

While we achieve approximately 70 % mixing for a T-mixer at $Re = 0.01$, complete mixing is achieved for the mixer with notches. This difference in mixing keeps increasing as *Re* increases. As the mixer design yields minimum mixing at $Re = 1$, while designing the length of these mixers for use in analytical systems, mixing at $Re = 1$ should be used as reference. If the mixer yields complete mixing at $Re = 1$ for the given length, then complete mixing will likely be achieved for $0.01 \leq Re \leq 100$ range for the same length.

4.2 Experimental Results

Apart from the optimized mixer a mixer with 50 μm wide notches, spaced 50 μm apart and going half way into the channel was also fabricated for further verification of the models. Figure 4 shows SEM images of the fabricated mixers. Experimental results of the optimized mixer and the mixer with 50 μm wide notches spaced 50 μm apart are shown in Figure 5. These results are in good agreement with the simulated ones, indicating >90% mixing within 7 mm at $Re = 0.1$, making the design ideal for LOC applications where space is limited. A representative experimental result of the fabricated micromixer with cross-section images taken at different distances from the

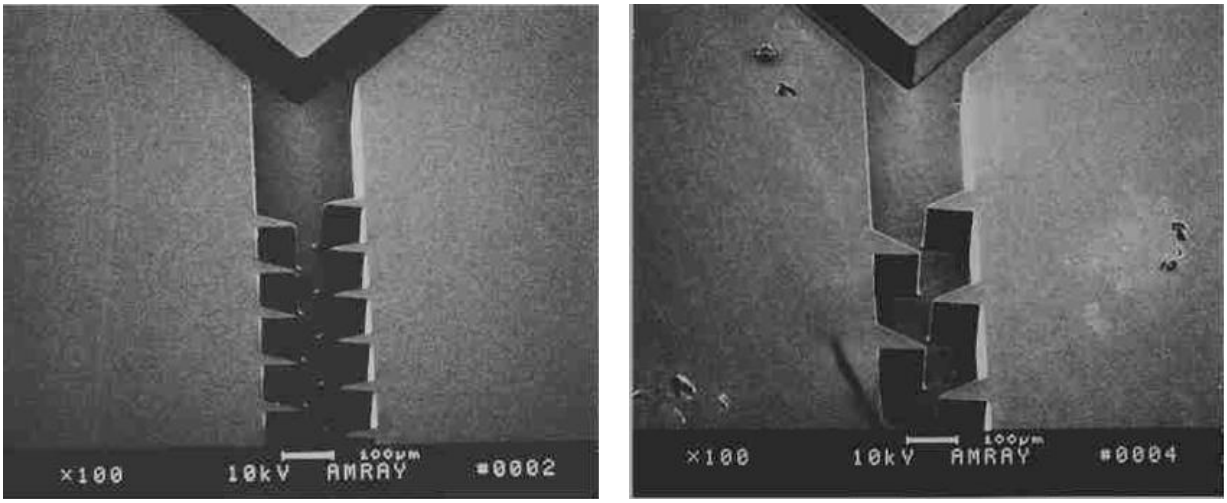

(a) **(b)**

Figure 4. Scanning electron micrographs of the notches micromixer in PDMS, (*a*) mixer with 25 µm wide notches with 25 µm spacing between them, (*b*) mixer with 50 µm wide notches with 50 µm spacing between them. Channel dimensions are 200 µm × 55 µm (W × H).

channel entrance at $Re = 0.1$ is shown in Figure 6. Although we intended to test the optimized mixer for $0.01 \leq Re \leq 100$ range, due to equipment limitation it could be tested for $0.02 \leq Re \leq 10$ only. For $Re < 0.02$, the syringe pump output resulted in a pulsating flow. Due to this, it was not possible to characterize the mixer for flows with $Re < 0.02$. Higher *Re* flows could not be tested due to the quality of the bonds between the PDMS molds and glass slides leading to device leakage. The plasma reactor used for oxygen bonding was not stable during the course of this work, and resulted in low quality bonding between PDMS and glass. Although the model predicted almost complete mixing for *Re* varying from 0.01 to 100, experimentally it could not be verified (Figure 7). One possibility for this discrepancy between the modeled and experimental results is that the fabricated notches were not identical to the ones modeled. The notches fabricated in PDMS do not go half way into the channel and are not terminated at a sharp point as modeled. The fabricated notches were ~90 µm in length rather than 100 µm. Thus there was a 20 µm width in the center of the channel where no features were present. Another reason for this difference between the experimental and modeled results was possibly the absence of point terminated notches. During modeling it was observed that the vortices formed at these sharp corners enhanced mixing, while the fabricated notches had smooth corners at the end of the notches. These two fabrication limitations reason the disagreement between the modeled and experimental results.

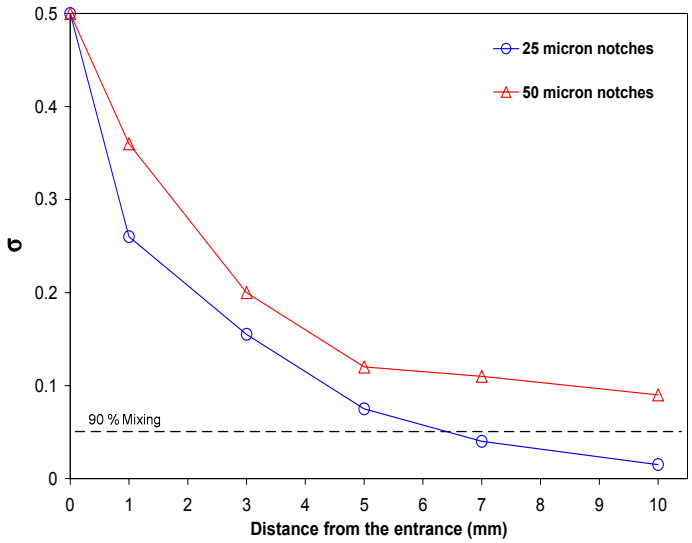

Figure 5. Experimental results for the 25 × 25 µm (width × spacing) and 50 × 50 µm notch mixers.

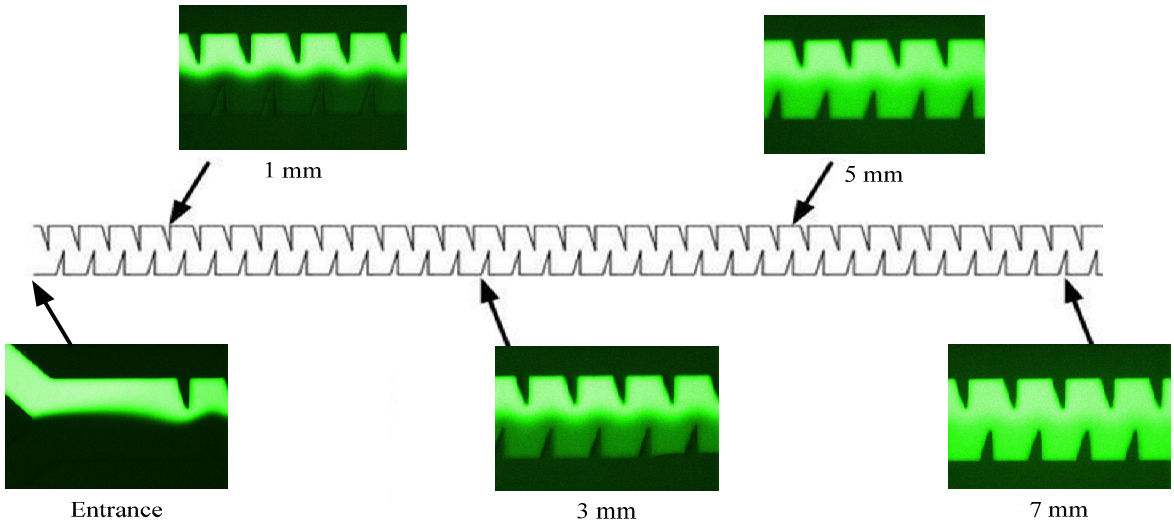

Figure 6. Experimental results indicating mixing at increasing distances from the channel entrance for the mixer with notches. Fluorescein is flowing in the upper (green) portion of the images and water in the lower portion.

5. CONCLUSIONS

In this paper a new passive micromixer with patterned sidewall notches is introduced. A detailed study of the effect of notches on mixing was carried out using the CFD-ACE+ software. Depending on the amount of mixing needed, one can easily pick the design they need for their application by varying the three control parameters indicated for the design. After analyzing the simulation results, an optimized mixer was then fabricated in PDMS from SU-8 molds. For lower *Re* the experimental results were in agreement with the simulations, while for higher *Re,* results did not correlate with the simulations due to fabrication limitations. The mixer achieves complete mixing within 7 mm for *Re* = 0.1. The advantage of using our design when compared to the others reported to date is the ease of fabrication since it does not involve any 3-D structures in the channel. The notches are all full channel height, can be patterned using a single lithography step, and require no alignment. Also the pressure drop along the channel is not

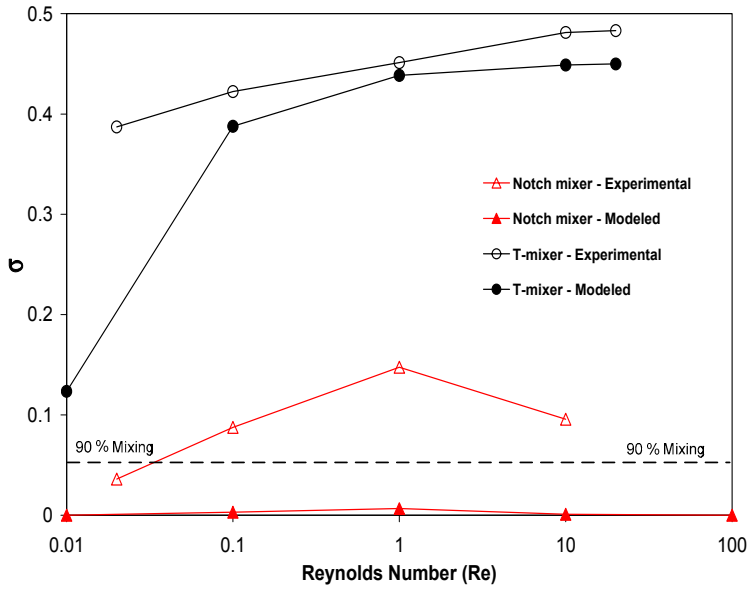

Figure 7. Experimental and modeled results for the optimized mixer for varying *Re* at 5 mm from the channel entrance. The notches are 25 μm wide and spaced 25 μm apart and go half way into the channel. The mixer performance is benchmarked against a conventional T-mixer

significant, which is an important factor to be considered while incorporating micromixers into LOC devices for applications requiring cascading of these mixers. These advantages make our design a good choice for an efficient micromixer for μTAS and LOC fields for chemical and biological analysis where space is limited.

ACKNOWLEDGEMENTS

This work was supported by a grant from the National Science Foundation (BES-0428600) and the University of Cincinnati Research Council Summer Graduate Student Research Fellowship. The authors are also grateful to Dr. Carl Seliskar for the use of his microscope facilities.

REFERENCES

1. J.Knight, "Honey, I shrunk the lab," *Nature*, vol. 418, pp. 474-475, 2002.
2. M. Freemantle, "Downsizing Chemistry," *Chemical and Engineering News*, vol. 8, pp. 27-36, Feb. 1999.
3. S. Borman, "Microchips Deliver on Command," *Chemical and Engineering News*, vol. 5, pp. 30-31, Feb. 1999.
4. A.G. Hadd, D. E. Raymond, J. W. Halliwell, S. C. Jacobson, and J. M. Ramsey, "Microchip device for performing enzyme assays," *Anal. Chem*., vol. 69, pp. 3407-3412, 1997.
5. S.C. Jacobson, and J.M. Ramsey, "Integrated microdevice for DNA restriction fragment analysis," *Anal. Chem*., vol. 68, pp. 720-723, 1996.
6. I. Kheterpal, and R.A. Mathies, "Capillary array electrophoresis DNA sequencing," *Anal. Chem*., vol. 71, pp. 31A-37A, 1999.
7. J. Khandurina, T. E McKnight, S. C. Jacobson, L. C. Waters, R. S. Foote, and J. M. Ramsey, "Integrated system for rapid PCR-based DNA analysis in microfluidic devices," *Anal. Chem*., vol. 72, pp. 2995-3000, 2000.
8. M. Kopp, A.D. Mello, and A. Manz, "Chemical amplification: continuous-flow PCR on a chip," *Science*, vol. 280, pp. 1046-1048, 1998.
9. P. Belgrader, M. Okuzumi, F. Pourahmadi, D. A. Borkholder, and M. A. Northrup, "A microfluidic cartridge to prepare spores for PCR analysis," *Biosensors and Bioelectronics*, vol. 14, pp. 849-852, 2000.
10. D.J. Harrison, K. Fluri, K. Seiler, Z. Fan, C. S. Effenhauser, and A. Manz, "Micromachining a miniaturized capillary electrophoresis-based chemical analysis system on a chip," *Science*, vol. 261, pp. 895-897, 1993.
11. S.B. Cheng, C. D. Skinner, J. Taylor, S. Attiya, W. E. Lee, G. Picelli, and J. D. Harrison, "Development of a multichannel micro fluidic analysis system employing affinity capillary electrophoresis for immunoassay," *Anal. Chem*., vol.73, pp. 1472-1479, 2001.
12. L.C. Waters, S. C. Jacobson, N. Kroutchinina, J. Khandurina, R. S. Foote, and M. J. Ramsey, "Microchip device for cell lysis, multiplex PCR amplification and electrophoretic sizing," *Anal. Chem*., vol. 70, pp. 158-162, 1998.
13. J. Yang, Y. Huang, X. B. Wang, F. F. Becker, and P. R. C. Gascoyne, "Cell separation on microfabricated electrodes using dielectrophoretic/gravitational field-flow fractionation," *Anal. Chem*., vol. 71, pp. 911-918, 2001.
14. A. Folch, B. H. Jo, O. Hurtado, D. J. Beebe, and M. Toner, "Microfabricated elastomeric stencils for micropatterning cell cultures," *J. Biomedical Materials Research*, vol. 52, pp. 346-353, 2000.
15. N. Nguyen, and Z. Wu, "Micromixers-a review," *J. Micromech. Microeng*., vol. 5, pp R1-R16, 2005.
16. J. Branebjerg, P. Gravesen, J. P. Krog, and C. Rye Nielsen, "Fast mixing by lamination," *Proc. 9th IEEE MEMS Workshop*, eds. M. G. Allen and M. L. Reed, San Diego, pp. 441-446, 1996.
17. R. H Liu, M. A. Stremler, K.V. Sharp, M. G. Olsen, J.G. Santiago, R. J. Adrian, H. Aref, and D. J. Beebe, "Passive mixing in a three-dimensional serpentine microchannel," *J. Microelectromech. Syst*., vol. 9, pp190-197, 2000.
18. A. D. Stroock, S. K. W. Dertinger, A. Adjari, I. Mezic, H. A. Stone, and G. M. Whitesides, "Chaotic mixer for microchannels," *Science*, vol. 295, pp 647-651, 2002.
19. D. S. Kim, S. W. Lee, T. H. Kwon, and S. S. Lee, "A barrier embedded chaotic micromixer," *J. Micromech. Microeng*., vol. 14, 798-805, 2004.
20. C. C. Hong, J-W. Choi, and C. H. Ahn, "A novel in-plane passive microfluidic mixer with modified Tesla structures," *Lab on a Chip*, vol. 4, pp 109-113, 2004.

21. T. Panitz, and D. T. Wasan, "Flow attachment to solid surfaces: The Coanda effect," *AIChE Journal*, vol. 18, pp 51-57, 1972.
22. J. Branebjerg, B. Fabius, P. Gravesen, "Application of miniature analyzers: From microfluidic components to μTAS," *Proc. Micro Total Anal. Syst. Workshop*, Enschede, The Netherlands, pp. 141-151, 1994.
23. B. H. Jo, L. M. Van Lerberghe, K. M. Motsegood, D. J. Beebe, "Three-dimensional micro-channel fabrication in polydimethylsiloxane (PDMS) elastomer," *J. Microelectromech. Syst*., vol. 9, pp. 76-81, 2000.
24. D. Simon, "Microscale flow visualization," *Microfluidics and Nanofluidics*, vol. 1, pp. 2-21, 2004.